Tris(indenyl)lanthanoid Complexes (Ln = La, Pr, Nd) Containing either (*S*)-(−)-Nicotine or Two Simpler Pyridine Bases

Jingwen Guan[a,b] and R. Dieter Fischer*[a]

Keywords: Lanthanides / N ligands / Chirality

Novel examples of the complex of the type [Ln(Ind)$_3$·Nic] [Ind = indenyl; Nic = (*S*)-(–)-nicotine] with Ln = La (**2**), Pr (**3**), and Nd (**4**) have been synthesised, along with their "parent" system [LaCp$_3$·Nic] (**1**). Complexes **2**–**4** were structurally, exhaustively characterised (XRS, ^{1}H NMR spectroscopy). Attempts to prepare homologues of **3** with achiral N-bases, pyridine, α-picoline, β-picoline, 2,6-dimethylpyridine, 2,6-bis(*tert*-butyl)pyridine, 2,2′-bipyridine, and 4,4′-dimethyl-2,2′-bipyridine, were successful with only the two least bulky bases, pyridine and β-picoline, which afforded the new adducts **5** and **6**, respectively. The chiral [Ln(Ind)$_3$·Nic] adducts are virtually isostructural, although subtle but systematic conformational variations emerge from the crystal structure analyses. While the unit cells of **2**–**4** contain two epimeric diastereomers, those of **5** and **6** involve genuine optical antipodes. The chiral carbon atom of nicotine lies approximately twice as far from the metal centre than the chiral sulfur atom of the methyl tolyl sulfoxide (MTSO) ligand in the previously reported [Ln(Ind)$_3$·MTSO] systems. As a result of this, the impact of the chiral MTSO ligand, both on the molecular structure and the ^{1}H NMR spectra, is found to be notably stronger than that of (*S*)-(–)-nicotine. The comparatively weak f-f circular dichroism of **3** is also compared with that of its (*S*)-(–)-MTSO-containing congener.

Introduction

Whilst the crystal structures of a few 1:1 adducts of a tris(cyclopentadienyl)lanthanoid(III) complex and pyridine (Py), or any pyridine derivative (Py*), have already been reported,[1−3] only one corresponding indenyl complex [Ce(Ind)$_3$·Py][4] has so far been characterised, also by X-ray crystallography. Structural studies on adducts containing the *chiral* pyridine derivative (*S*)-(−)-nicotine (Nic) are yet to be reported on, although several [LnCp$_3$·Nic] systems were prepared for early spectroscopic studies.[5,6]

Our current interest in the structural details of diverse [(Ind)$_3$Ln·Py*] systems results from more recent observations in which the three bulky benzo groups of the indenyl units may be oriented in various different ways[7−9] depending on the actual bulkiness of the metal-coordinated Lewis base. Moreover, a *chiral* Lewis base L is also expected to control the chirality of the {Ln(Ind)$_3$X} fragment[7] (X is the ligand atom that is bonded to the metal centre), provided that the chiral centre of the base resides only two bonds away from the metal centre, as in chiral sulfoxides[10] and 2-methyltetrahydrofuran.[11a] In the present study, our interest will be focused on whether a chiral centre located about twice as far from the metal centre than that in the recently investigated methyl tolyl sulfoxide (MTSO) adducts,[10] would still exert any detectable configuration controlling or electronic influence. While the chiral sulfur atom of the oxygen-coordinated MTSO ligand is separated from the metal ion by only one atom, three atoms would separate the chiral carbon atom of a *nicotine* ligand (coordinated via its pyridine N atom) from the metal centre (see Figure 1). Particular attention will therefore be paid to subtle conformational details in the crystal structures, to auxiliary ^{1}H NMR signal displacement or splitting effects due to the presence of paramagnetic metal ions, and even to potential f-f circular dichroism of the central Ln^{III} ions with an incomplete 4f^q configuration. We thus wish to present an exemplary description of the employment of suitable alternative techniques, in combination with X-ray crystallography, to elucidate the influence of paramagnetic 4f^q metal ions on distinct features of the ligand sphere, and, conversely, of notably remote chirogenic centres on the 4f electrons. In addition we report on the first successful synthesis of analytically pure [Ln(Ind)$_3$·Nic] compounds (Ln = La, Pr, Nd).

Results and Discussion

Synthesis and General Properties of [La(C$_5$H$_5$)$_3$·Nic] (1)

Facile ligand exchange was found to take place, when a solution of (*S*)-(−)-nicotine in toluene was added to a suspension of [La(C$_5$H$_5$)$_3$·THF][8] in toluene. The product precipitated as a faint yellow powder which dissolves readily in CH_2Cl_2 and THF, but only moderately in benzene or toluene. In THF the reverse reaction of Equation (1) was found to occur. In the mass spectrum, both metal-containing [Cp$_n$La]$^+$ fragments with n = 3, 2, 1, 0, and smaller purely organic fragments of nicotine were observed. In the ^{139}La NMR spectrum, one relatively broad resonance at δ = −534 ($w_{1/2}$ = 979 Hz), referenced to a solution of $LaCl_3$ in

[a] Institut für Anorganische und Angewandte Chemie der Universität Hamburg,
Martin-Luther-King-Platz 6, 20146 Hamburg, Germany
Fax: (internat.) + 49-40/42838−2882
E-mail: fischer@chemie.uni-hamburg.de
[b] Department of Chemistry, University of Ottawa,
Ottawa, Ontario, Canada

  1434−1948/01/1010−2497 $ 17.50+.50/0

D_2O, appears. This compares reasonably with corresponding results for $[La(C_5H_5)_3{\cdot}THF]$ ($\delta = -558$, 450 Hz) and $[La(C_5H_5)_3{\cdot}MTSO]$ ($\delta = -563$, 390 Hz).[8,10] In the ^1H NMR spectrum of **1**, *all* the resonances for the nicotine protons were assigned in a similar manner to those in the ^1H NMR spectrum of a previously reported paramagnetic $[PrCp_3{\cdot}Nic]$ complex.[6] However, several lines in the ^1H NMR spectrum of **1** are overlapping. For the full assignment of the spectroscopic results (see Exp. Sect.), the designation of the nicotine protons is adopted as given in Figure 1. While the ^1H NMR spectrum of the paramagnetic Pr^{III} complex had already revealed that the nicotine molecule is coordinated via its pyridine N atom,[6] this particular feature is not as convincingly apparent from the spectrum of diamagnetic **1**.

$$[La(C_5H_5)_3{\cdot}THF] + \text{(S)-(-)-nicotine} \xrightarrow{\textit{toluene}} [La(C_5H_5)_3{\cdot}Nic]\ (\mathbf{1}) + THF \quad (1)$$

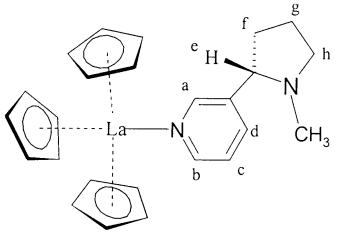

Figure 1. Schematic structure of complex **1**, including the designation of the protons on the nicotine ligand

Synthesis and General Properties of the $[Ln(Ind)_3{\cdot}Nic]$ Systems 2−4 (Ln = La, Pr, Nd)

The three nicotine adducts $[Ln(Ind)_3{\cdot}Nic]$ with Ln = La, Pr, and Nd (**2**−**4**) could be obtained similarly, by ligand exchange reactions, i.e. by adding a solution of nicotine in toluene, to a suspension of the corresponding THF adduct $[Ln(Ind)_3{\cdot}THF]$ as shown in Equation (2). Somewhat unexpectedly, all tris(indenyl) homologues of **1** resulted in viscous oils which are analytically pure. However, when the yellow-orange oil of **2** coexisted with a trace amount of toluene, the sticky syrup converted overnight into rod-like, bright yellow crystals of excellent X-ray quality. However, this simple technique was not suitable for the crystallisation of **3** and **4**. Crystals of the latter complexes could only be obtained when the viscous oils were first dissolved in small amounts of toluene, after which a large amount of hexane was slowly added. After some time, crystal-like products could be seen. Finally, the liquid phase was decanted, and the remaining solid was washed with hexane. The purified residues were redissolved in hot toluene and the temperature was lowered very slowly and steadily. Prismatic leek-green crystals of **3**, and grass-green crystals of **4**, were obtained which were of excellent quality for X-ray crystallographic studies. Toluene solutions of these crystals no longer afforded the viscous oils after the removal of the solvent.

$$[Ln(C_9H_7)_3{\cdot}THF] + \text{(S)-(-)-nicotine} \xrightarrow{\textit{toluene}} [Ln(C_9H_7)_3{\cdot}\text{(S)-nicotine}] + THF \quad (2)$$
$$Ln = La, Pr \text{ and } Nd$$

Complexes **2**−**4** are very soluble in toluene, benzene, THF, MeCN, and CH_2Cl_2, but insoluble in hexane. The nicotine adducts appear to be thermally more stable (under N_2) than their corresponding MTSO congeners.[10] In the mass spectra of all three complexes, signals corresponding to the metal-containing fragments $[Ind_nLn]^+$ with $n = 3$, 2, 1, and 0 were found. Several weaker peaks assigned to purely organic fragments such as $[Ind]^+$, $[Nic]^+$, $[C_5H_4NC_4H_7]^+$, $[C_5H_4NC_3H_5]^+$, $[C_4H_7NCH_3]^+$, etc. were observed as well. Variable-temperature ^{139}La NMR spectroscopic studies of **2** show that the signal is considerably broadened with decreasing temperature. Interestingly, this broadening effect seems to be notably more pronounced for tris(indenyl)- than for tris(cyclopentadienyl)lanthanum(III) complexes.[8] This suggests a more sensitive response of the large ^{139}La nuclear quadrupole moment on the presence of the less symmetrical (as compared with C_5H_5) indenyl ligands (see Table 1).

Table 1. Comparison of the ^{139}La NMR results (chemical shift and line width) for corresponding cyclopentadienyl and indenyl complexes $[LaCp'_3{\cdot}L]$ (Cp′= Cp or Ind)

L	Temp. [K]	δ(^{139}La) Cp	Ind	$w_{1/2}$ [Hz] Cp	Ind	Ref.
(*S*)-(−)-Nic	345	−534	−413	545	1221	
(*S*)-(−)-Nic	325	−535	−417	675	1695	
(*S*)-(−)-Nic	292	−539	−425	980	2765	
THF	320		−558		508	[8]
(*S*)-(−)-MTSO	320		−450		2480	[10]

Another interesting feature of the nicotine complexes **2**−**4** is that their melting points are quite low (**2**: 94−98; **3**: 129−132; **4**: 112−116 °C). Only the melting point of **3** compares with those of the reported $[Ln(Ind)_3{\cdot}MTSO]$ systems.[10] Possibly, the "tadpole-like" shape of a $[Ln(Ind)_3{\cdot}Nic]$ molecule, with its extended nicotine tail (vide infra), can undergo various facile conformational changes, which − with its pronounced flexibility − is likely to inhibit the arrival at a well-ordered crystalline phase.

Attempted Syntheses of Related $[Pr(Ind)_3{\cdot}Py^*]$ Adducts; Preparation and General Properties of $[Pr(Ind)_3{\cdot}Py]$ (5) and $[Pr(Ind)_3{\cdot}(3\text{-}MePy)]$ (6)

The corresponding pyridine and β-picoline adducts of complex **3** were prepared in a similar manner to complex **3** (Ln = Pr) as shown in Equation (3). In contrast to **2**−**4**, the simpler adducts **5** and **6** did not form viscous oils, but rather leek-green microcrystals formed, which could readily be recrystallised from hot toluene affording single crystals suitable for X-ray crystallography. Both compounds are reasonably soluble in toluene and benzene, but more soluble in MeCN, CH_2Cl_2, and THF. In the mass spectra, peaks of the metal-containing fragments $[Ind_nPr]^+$ with $n = 3$, 2, 1,

and the organic fragments $[Ind]^+$, $[Py]^+$, or $[MePy]^+$ were observed.

$$[Pr(Ind)_3{\cdot}THF] + Py^* \xrightarrow{toluene} [Pr(Ind)_3{\cdot}Py^*] + THF \quad (3)$$

Py^* = pyridine: **5**, 3-methylpyridine (β-picoline): **6**

^{1}H NMR spectroscopic data for the indenyl protons of **5** and **6** are included in Table 5, while the corresponding data for the protons of the Py* ligands are found in the Exp. Sect. Quite surprisingly, the chemical shifts of the H atoms next to the pyridine N atom, which are separated from the paramagnetic metal ion by one atom more than the indenyl H atoms, experience notably stronger "paramagnetic" displacements than the indenyl resonances.

Several attempts were made to vary the steric congestion of the potential ligand Py*, by changing the ring substituents and/or their positions on the pyridine fragment. Thus, the pyridine derivatives listed in Equation (4) were subjected to ligand (i.e. THF) exchange experiments, with the hope of initiating new conformational features in the final architecture of the expected complexes. However, all these preparative attempts remained unsuccessful, as the isolable leek-green, crystalline products turned out to be the starting compound $[Pr(Ind)_3{\cdot}THF]$ (as confirmed by elemental analysis, ^{1}H NMR spectroscopy, and crystal structure analysis).

$$[Pr(C_9H_7)_3{\cdot}THF] + Py^* \xrightarrow{toluene} \not\rightarrow [Pr(C_9H_7)_3{\cdot}Py^*] + THF \quad (4)$$

Py* = α-picoline, 2,6-dimethylpyridine, 2,6-bis(tert-butyl)pyridine
4,4'- dimethyl-2,2'-bipyridine and 2,2'-bipyridine

These results clearly indicate that just one methyl group in the 2-position of a pyridine molecule (i.e. α-picoline) no longer allows the indenyl ligands to adopt orientations that would provide enough space for the coordination of this pyridine derivative. This observation does not agree with recent findings in which 2-methyltetrahydrofuran (MeTHF) readily bonds to $\{Ln(\eta^5\text{-}Ind)_3\}$ fragments.[11a] Moreover, one or two of the three indenyl ligands might in principle abandon their usual η^5 coordination for a lower hapticity. This has been suggested for the recently prepared complex $[Lu(C_9H_7)_3{\cdot}3THF]$, in view of its notably higher THF content,[11b] and also for the well-documented crystalline $[LuCp_3]$ complex which has an η^1-coordinated Cp ligand.[12] The failure of α-picoline to enter the coordination sphere of a $\{Pr(Ind)_3\}$ fragment indicates that the required change from η^5 to η^1 (or η^3) coordination probably needs some auxiliary "support" to overcome the higher steric demand of the potential ligands listed in Equation (4).

Crystallographic Studies of the $[Ln(Ind)_3{\cdot}Nic]$ Complexes 2−4

Selected details of the data collection and structure refinement of **2**−**4** are listed in Table 7. Although the three complexes are virtually isostructural, their cell parameters differ significantly, suggesting at least some conformational variation (vide infra).

The C_5 fragments of the indenyl ligands are all η^5-coordinated, although the individual Ln−C distances vary considerably (Table 2). The nicotine ligand is bonded to the metal centre exclusively via its pyridine N atom. The unit cells of **2**, **3**, and **4** contain two rather similar-looking epimeric diastereomers (Figure 2). As the chiral carbon atom of the nicotine ligand lies relatively far from the metal centre, the chiral $\{Ln(Ind)_3{\cdot}N\}$ fragments for each epimeric pair behave as almost perfect mirror images. This situation strongly resembles that observed for several $[Ln(Ind)_3{\cdot}L]$ systems with an achiral L, e.g. L = THF (Ln = La or Pr),[8] L = diphenyl sulfoxide, DPSO (Ln = Nd),[10] and L = Py or β-MePy (Ln = Pr, i.e. in **5** and **6**, vide infra). Here, the unit cell of the crystal always involves both enantiomers (1:1) of a chiral $\{Ln(Ind)_3X\}$ fragment (X = either O or N). On the other hand, in the single crystals of the very closely related adducts $[Ln(Ind)_3{\cdot}L]$ with L = THF (Ln = Sm, Tm[8] and Gd[13]), and L = either (*R*)-(+)- or (*S*)-(−)-MTSO (Ln = La or Pr[10]), only one distinct $\{Ln(Ind)_3{\cdot}X\}$ enantiomer is present.

Initially, the evidence suggested that the three homologues crystallise in the centrosymmetric space group $P2_1/c$. However, after careful assessment of the systematic absence of numerous weak reflections, and along with the non-vanishing chirality of each metal complex, there is no doubt that all three homologues crystallise in the acentric and chiral space group $P2_1$. In Figure 2, the molecular structures of the three epimeric pairs of **2**, **3**, and **4** are depicted such that the orientation of their Ln1−N1−C33 and Ln2−N3−C43 vectors have been kept unchanged. While this particular view was chosen to demonstrate that large portions of each epimeric pair of molecules behave as mirror images, the two diastereomers are positioned face-to-face in the crystals of **2** and **3** (i.e. their nicotine tails turn away from each other), but back-to-back in the lattice of **4**. In all of the structures displayed in Figure 2, the methylated pyrrolidine N atom prefers just one distinct configuration. However, with respect to rotation about the ring-ring C−C bond, the two cyclic components of the nicotine ligand of **4** adopt another conformation than in **2** and **3**.

Selected bond lengths and angles of **2**, **3** and **4** are listed in Table 2. The Ln−C distances involving carbon atoms shared by the C_5 *and* C_6 units of each indenyl ligand are, as usual, significantly longer than the other Ln−C bonds of each C_5 fragment. The Ln−N distances compare well with that reported for $[Ce(C_9H_7)_3{\cdot}Py]$ [Ce−N 268.4(4) pm],[4] and are also in agreement with those in $[Nd(C_5H_5)_3{\cdot}Py]$ [266.8(5)] and in $[Sm(C_5H_5)_3{\cdot}Py]$ [265.6(3) pm].[2] Interestingly, these Ln−N distances are longer than the Ln−O distances in the corresponding $[Ln(Ind)_3{\cdot}MTSO]$ systems,[10] by about 20 pm. The Ce−N distance in $[Ce(MeC_5H_4)_3{\cdot}N(CH_2CH_2)_3CH]$ [278.6(4) pm] exceeds the aforementioned Ln−N distances by at least 10 pm.[14] Intramolecular Nd−N distances ≥ 280 pm are also reported for $[Nd(C_5H_4CH_2CH_2NMe_2)_2Cl]$ and $[Nd(C_5H_4CH_2CH_2NMe_2)_3]$[15,16] while the Nd−N(Py) distances are about 268 pm.[17]

The various molecular conformations, with respect to η^5-indenyl rotation about the individual Ln−Ct*i*5 axes (Ct15, Ct25, and Ct35 being the centres of the three C_5 fragments), of the diastereomers of crystalline **2**, **3**, and **4** may be quan-

Table 2. Selected bond lengths [pm] and angles [°] of the nicotine complexes **2**−**4**; data in italics refer to slightly more elongated Ln−C distances (see text)

	2	**3**	**4**
Bond lengths			
Ln−N(1)/(3)	265.7(6)/269.0(7)	270.8(9)/262.9(11)	265(3)/268(2)
Ln−C(101)/(201)	287.3(6)/283.6(6)	275.6(9)/286.2(11)	281(3)/274(3)
Ln−C(102)/(202)	283.1(6)/282.2(5)	278.6(11)/277.9(11)	278(2)/268(2)
Ln−C(103)/(203)	286.0(7)/289.2(6)	289.1(10)/277.7(10)	273(3)/286(2)
Ln−C(108)/(208)	*303.3(7)/303.6(7)*	*291.4(9)/299.7(10)*	*300(2)/290(3)*
Ln−C(109)/(209)	*303.1(8)/306.4(7)*	*301.8(10)/294.5(9)*	*296(2)/295(3)*
Ln−Ct(15)	266.5/267.0	260.9/260.7	258.5/255.9
Ln−C(111)/(211)	283.4(8)/289.3(7)	278.7(10)/280.1(12)	281(2)/285(3)
Ln−C(112)/(212)	284.8(9)/286.4(8)	280.0(11)/278.3(10)	272(3)/267(3)
Ln−C(113)/(213)	286.8(7)/283.0(8)	280.4(10)/281.4(10)	274(3)/280(3)
Ln−C(118)/(218)	*287.4(7)/290.0(7)*	*290.7(11)/294.8(10)*	*301(2)/303(3)*
Ln−C(119)/(219)	*288.3(7)/286.3(7)*	*292.2(11)/291.0(11)*	*287(2)/292(3)*
Ln−Ct(25)	259.3/260.5	257.2/258.7	256.1/259.1
Ln−C(121)/(221)	283.1(8)/281.9(8)	279.2(11)/276.4(11)	273(2)/267(3)
Ln−C(122)/(222)	282.8(7)/284.9(7)	278.4(10)/279.5(10)	274(3)/271(2)
Ln−C(123)/(223)	290.3(6)/291.2(7)	279.6(11)/281.5(10)	273(2)/288(2)
Ln−C(128)/(228)	*292.9(7)/290.5(6)*	*284.8(11)/280.5(11)*	*295(3)/290(2)*
Ln−C(129)/(229)	*297.5(6)/295.4(6)*	*286.7(10)/284.5(10)*	*294(3)/300(2)*
Ln−Ct(35)	262.7/262.5	253.8/254.0	255.9/256.9
Angles			
N−Ln−Ct(15)	102.1/120.7	104.5/105.3	109.3/98.3
N−Ln−Ct(25)	98.1/96.1	92.0/92.0	92.5/104.1
N−Ln−Ct(35)	97.1/98.6	100.8/100.2	98.8/94.9
Ct(15)−Ln−Ct(25)	114.4/114.0	118.2/118.0	115.9/115.8
Ct(25)−Ln−Ct(35)	117.4/117.9	117.4/117.6	120.3/116.1
Ct(35)−Ln−Ct(15)	120.6/120.6	117.0/116.9	114.8/120.7
Ct(16)−Ct(15)−Ct(35)	74.7/75.1	79.2/80.0	77.9/70.0
Ct(16)−Ct(15)−Ct(25)	133.5/133.7	126.6/126.8	130.8/125.2
Ct(26)−Ct(25)−Ct(15)	83.9/84.3	70.5/71.6	78.1/76.7
Ct(26)−Ct(25)−Ct(35)	83.4/83.1	127.0/127.2	127.4/132.2
Ct(36)−Ct(35)−Ct(25)	114.1/111.7	85.5/84.9	70.8/78.4
Ct(36)−Ct(35)−Ct(15)	89.8/90.3	84.1/83.7	125.5/127.3
Ct(16)−Ct(15)−Ln	101.5/101.2	98.4/98.7	100.2/99.7
Ct(26)−Ct(25)−Ln	92.0/91.9	96.0/96.5	98.9/101.1
Ct(36)−Ct(35)−Ln	94.7/93.7	93.2/92.7	100.6/99.5

tified by inspecting the distances of the three C_6 ring centres, Ct*i*6 (i = 1−3), from the best plane spanned by the three C_5 ring centres, Ct*i*5.[8,10] These quantities, along with the distance of the metal ion from the Ct15/Ct25/Ct35 plane, are listed in Table 3 for the complexes **2**−**7**. The second digit of the individual number of each indenyl carbon atom as found in Figure 2 (i.e. 0, 1, or 2), corresponds to the indenyl ring number *i* (1, 2, or 3) used in Table 3.

For an ideal paddlewheel-like conformation (the benzo groups are considered as "paddles"), with three *equatorially* oriented indenyl ligands, the Ct*i*6-to-plane distances should be minimal (i.e. ≤ 10 pm), whilst the ideal distance for *meridionally* oriented indenyl ligands should be ca. 220 pm.[10] The term "approximately *equatorial*" may be used for distances up to 150 pm, and the term "approximately *meridional*" may be used for distances > 150 pm. By this classification, complex **2** would have two, complex **3** one, and complex **4** no indenyl ligands of *meridional* orientation. This classification agrees well with earlier findings in which the paddlewheel-like conformation is gradually favoured as the radius of the metal ion decreases.[8,10] The opposite signs of the Ct*i*6-to-plane distances of the two meridional ligands of **2** (with i = 2 and 3) indicate that one of the two indenyl benzo groups is located *trans* to the nicotine ligand, and the other one *cis*. While the Ct*i*6-to-plane distances of the two diastereomers of **2** do not differ significantly, the corresponding data sets of **4** display more pronounced deviations. For instance, the Ct16- and Ct36-to-plane values of the two diastereomers have opposite signs. In view of these findings, the two {Nd(Ind)$_3$·N} fragments of **4** (see Figure 2), cannot even be considered as "approximate" mirror images.

Crystallographic Studies of [Pr(Ind)$_3$·Py] 5 and [Pr(Ind)$_3$·(3-MePy)] (6)

Crystals of the two complexes [Pr(Ind)$_3$·Py] (**5**) and [Pr(Ind)$_3$·3-MePy] (**6**) are orthorhombic and belong to the cubic space group *Pbca*. This can be seen in Table 8. Corresponding properties are reported for the cerium homologue [Ce(Ind)$_3$·Py] (**7**).[4] As the unit cell parameters of **5**, **6**, and **7** are similar, the three complexes are quasi-isostructural, although their molecular conformations may still

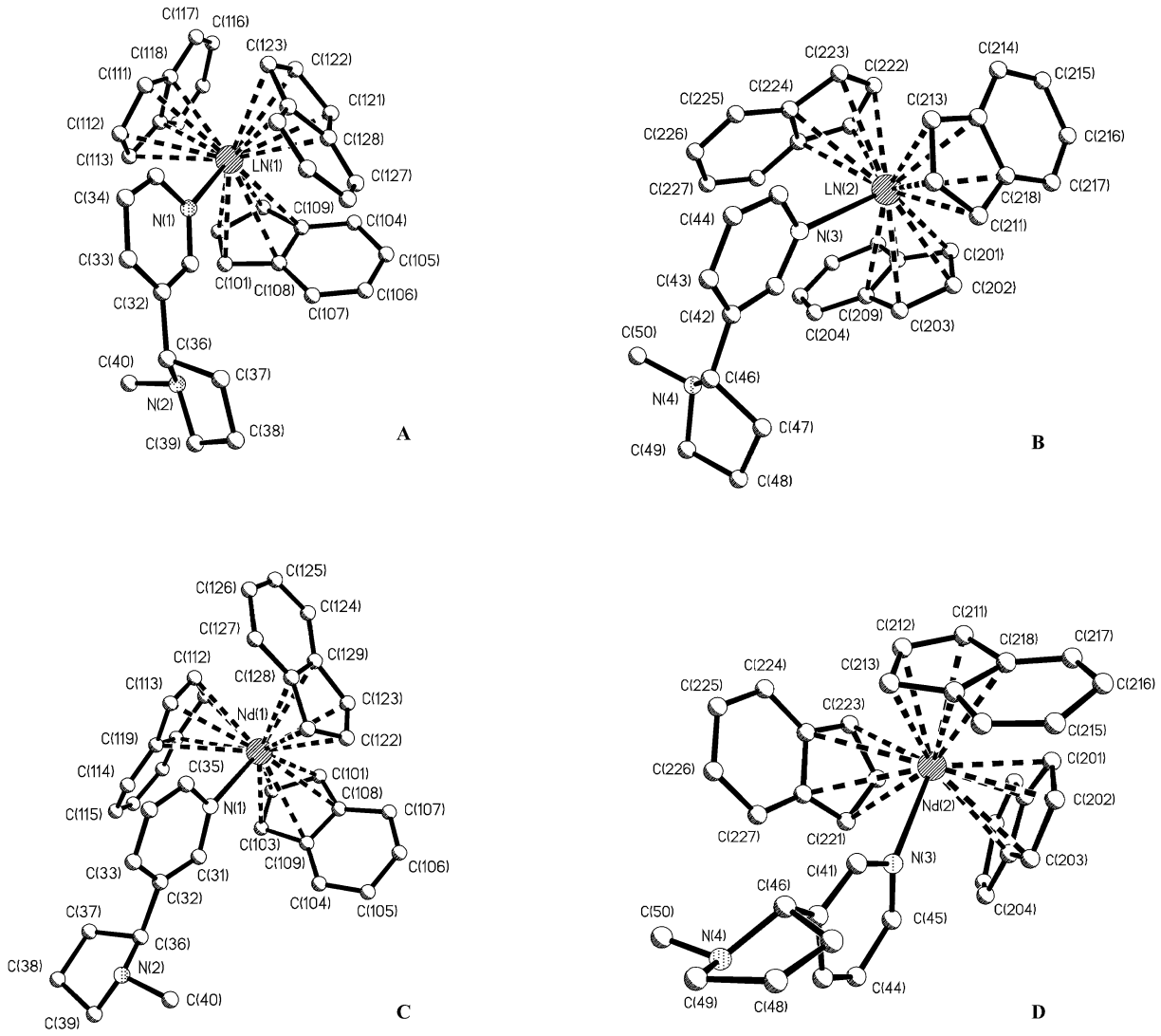

Figure 2. Molecular structure and atomic numbering scheme of the two epimeric diastereomers of **2** and **3** (**A/B**), and **4** (**C/D**), respectively; the drawings **A/B** refer to **2**, although **2** and **3** are almost isostructural; for the specific, pairwise orientation see the text

Table 3. Distances of the C_6 centers Ct*i*6 (i = 1−3), and the metal atom Ln, from the best plane spanned by the three C_5 centres, Ct*i*5, of each epimeric or racemic pair of **2**−**7** (distances in pm; a negative sign indicates the disposal of Ct*i*6 *transoid* to Py*)

Sample	Ln	Ct16	Ct26	Ct36
2 (La)	42.4/42.0	23.4/35.2	−216.4/−217.3	192.1/198.2
3 (Pr)	40.8/41.2	122.8/127.2	66.9/73.6	−218.6/−217.9
4 (Nd)	44.9/40.5	103.3/−78.1	109.6/83.1	−81.8/114.8
5 (Pr)	44.4	−107.1	113.2	113.1
6 (Pr)	50.0	153.9	152.5	88.2
7 (Ce)[4]	45.2	−106.5	113.9	114.2

vary. The molecular structures of **5** and **6** are shown in Figure 3. As the conformations of both complexes are approximately paddlewheel-like (vide supra) (Table 3), the {Ln(Ind)$_3$N} fragments are chiral. The crystal lattices of all three adducts with achiral Py* ligands involve racemic mixtures of molecules with both clockwise and anticlockwise (with respect to the Ln−N axis) oriented benzo groups.

Selected bond lengths and angles are listed in Table 4. The Pr−N distances again compare well with those of **7**[4] and with those of all other [Ln(Ind)$_3$·Py*] systems mentioned above. The Pr−C bond lengths vary between 273.8(4) and 301.8(4) pm, which is a feature also reported for **7**.[4]

Although the conformations of **5** and **6** are paddlewheel-like (like that of **4**), a closer look at the Ct*i*6-to-plane distances listed in Table 3 reveals that the data for **5** satisfactorily match with only one set of **4**. No counterpart exists for a set of three positive Ct*i*6 values (as actually found for **6**).

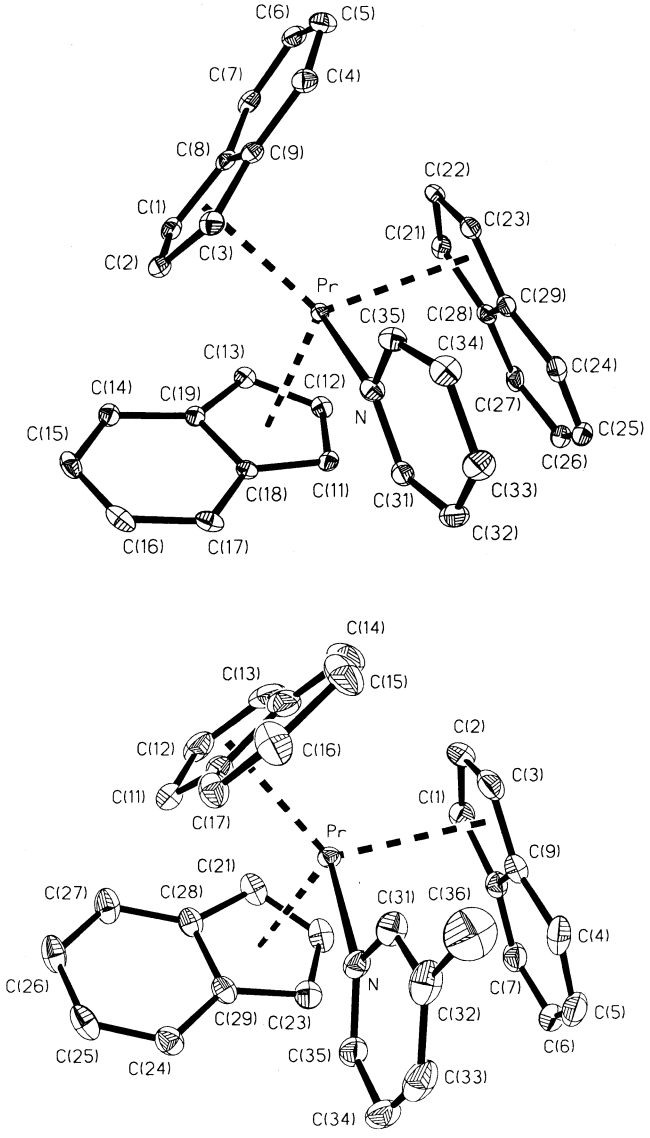

Figure 3. Molecular structure and atomic numbering scheme of the complexes **5** (top) and **6** (bottom)

Table 4. Selected bond lengths [pm] and angles [°] of **5** and **6**; data in italics refer to slightly more elongated Ln−C distances (see text)

Bond lengths	**5**	**6**	Angles	**5**	**6**
Ln−N	266.9(3)	260.8(3)	N−Ln −Ct(15)	103.8	96.2
Ln−C(1)	275.7(3)	278.7(4)	N−Ln−Ct(25)	104.1	104.3
Ln−C(2)	274.3(4)	275.2(4)	N−Ln−Ct(35)	91.8	103.1
Ln−C(3)	285.3(3)	280.0(4)	Ct(15)−Ln−Ct(25)	116.0	118.3
Ln−C(8)	*293.3(3)*	*291.7(4)*	Ct(25)−Ln−Ct(35)	118.1	114.2
Ln−C(9)	*301.0(3)*	*292.9(4)*	Ct(35)−Ln−Ct(15)	117.3	116.5
Ln−Ct(15)	259.1	256.9	Ct(16)−Ct(15)−Ct(35)	69.7	83.4
Ln−C(11)	275.1(3)	277.7(4)	Ct(26)−Ct(25)−Ct(15)	76.1	87.3
Ln−C(12)	276.4(3)	273.8(4)	Ct(36)−Ct(35)−Ct(25)	78.4	76.2
Ln−C(13)	283.9(3)	279.1(5)	Ct(16)−Ct(15)−Pr	76.1	96.4
Ln−C(18)	*289.1(3)*	*293.9(4)*	Ct(26)−Ct(25)−Pr	97.0	99.4
Ln−C(19)	*296.2(3)*	*295.2(1)*	Ct(36)−Ct(35)−Pr	98.2	99.6
Ln−Ct(25)	257.1	257.0			
Ln−C(21)	280.0(3)	285.9(4)			
Ln−C(22)	274.0(3)	275.6(5)			
Ln−C(23)	277.8(3)	277.2(5)			
Ln−C(28)	*296.8(3)*	*301.8(4)*			
Ln−C(29)	*294.9(3)*	*294.3(4)*			
Ln−Ct(35)	257.8	260.5			

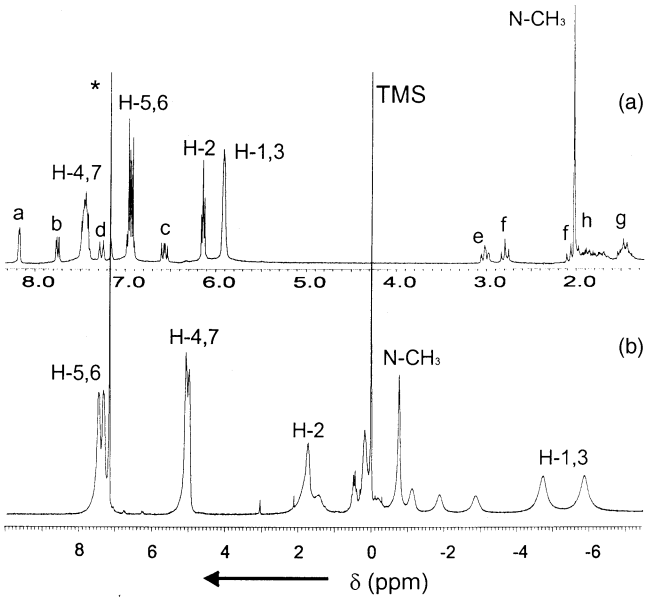

Figure 4. Room-temperature ^{1}H NMR spectra of **2** (a) and **4** (b); solvent: C_6D_6/TMS; signals of the indenyl protons are marked by asterisks; two resonances of **4** (beyond δ = −10, see Exp. Sect.) are not shown

Solution ^{1}H NMR Spectroscopy of 2, 3, and 4

The ^{1}H NMR spectrum of diamagnetic **2** (Figure 4, a) displays almost the same resonance pattern, with respect to the protons of its nicotine ligand, as the spectrum of **1** (see Exp. Sect.). The resonance pattern of the indenyl protons of **2** is consistent with the presence of three virtually equivalent C_9H_7 units. As in the case of [La(Ind)$_3$·THF],[8] no more than four multiplets (I_{rel} = 6:6:3:6) occur indicating that the six pairwise prochiral[10] C_9H_7 protons (see Figure 5) do not experience any significant diastereotopic splitting due to the relatively remote location of the chiral carbon atom of the (*S*)-(−)-nicotine ligand. In striking contrast, however, the three equivalent C_9H_7 ligands of the complex [La(Ind)$_3$·MTSO] [with either (*R*)-(+)- or (*S*)-(−)-MTSO] were found to display *seven* equally intense (I_{rel} = 3) multiplets.[7,10]

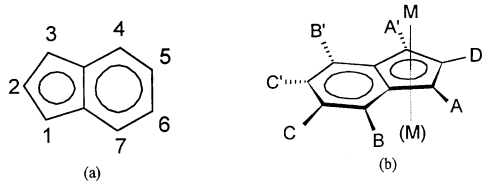

Figure 5. Conventional numbering of indenyl hydrogen atoms (a); schematic description of the prochiral nature of the atoms A/A′, B/B′ and C/C′ in an {M(η^n-indenyl)} fragment (b)

Table 5. Room-temperature chemical shifts (ppm) of the indenyl protons of various [Ln(Ind)$_3$·L] systems (solvent: C_6D_6; for the designation of the H atoms see Figure 5, a)

Ln	L	1/3-H	2-H	4/7-H	5/6-H
La	(*S*)-(−)-Nic (**2**)	5.90 (s, 6 H)	6.14 (t, 3 H)	7.46 (m,6 H)	6.94 (q,6 H)
Pr	(*S*)-(−)-Nic (**3**)	9.59 (s, 3 H); 8.79 (s, 3 H)	7.44 (s, 3 H)	8.15 (d, 3 H); 8.03 (d, 3 H)	4.19 (t, 3 H); 4.06 (t, 3 H)
Pr	Py (**5**)	10.03 (s, 6 H)	8.98 (s, 3 H)	7.88 (s, 6 H)	3.65 (s, 6 H)
Pr	3-MePy(**6**)	10.13 (s, 3 H)	7.66 (s, 3 H)	8.12 (s, 6 H)	3.68 (d, 6 H)
Pr	(*R*)-(+)-MTSO[10]	19.55 (s, 3 H); −0.52 (s, 3 H)	1.98 (s, 3 H)	10.41 (d, 3 H); 6.22 (d, 3 H)	4.95 (t, 3 H); 3.85 (t, 3 H)
Pr	DPSO[a] [10]	9.25 (s, 6 H)	4.16 (s, 3 H)	8.18 (q,6 H)	4.02 (dd,6 H)
Nd	(*S*)-(−)-Nic (**4**)	−4.73 (s, 3 H); −5.88 (s, 3 H)	1.74 (s, 3 H)[b]	7.40 (d, 6 H)[c]	5.00 (d, 6 H)[d]
Nd	(*R*)-(+)-MTSO[10]	−2.00 (s.3 H); −7.46 (s, 3 H)	6.09 (s, 3 H)	9.49 (s, 3 H); 6.10 (s, 3 H)	4.32 (s, 3 H); 3.30 (s, 3 H)
Nd	DPSO[a] [10]	−3.87 (s, 6 H)	−0.89 (s, 3 H)	7.66 (s, 6 H)	5.12 (s, 6 H)
Nd	TPPO[d] [11c]	−6.36 (s, 6 H)	−2.56 (s, 3 H)	7.27 (s, 6 H)	5.53 (s, 6 H)

[a] DPSO = diphenyl sulfoxide. − [b] With L = THF, δ(2-H) = 6.73, see ref.[8] − [c] Distance of the two components (in Hz): 480, ruling out any internuclear spin-spin coupling. − [d] TPPO = triphenylphosphane oxide (see also ref.[7]).

On the other hand, the expected diastereotopic splitting for L = (*S*)-(−)-nicotine (instead of MTSO) becomes observable in the ^{1}H NMR spectra of the *paramagnetic* homologues of **2** (i.e. of **3** and **4**) at room temperature. A survey of the relevant ^{1}H NMR spectroscopic data is given in Table 5. A detailed variable-temperature (VT) ^{1}H NMR study (between 353 and 188 K) of **3**, dissolved in [D_8]toluene, shows that the indenyl protons give rise to three singlets, two quasi-doublets and two quasi-triplets between ca. 320 and 260 K (see Figure 6, b, and Table 5). However, above room temperature (e.g. at 353 K, see Figure 6, a) the two quasi-doublets together with one of the singlets collapse to form one intense quasi-triplet, and the two initially present quasi-triplets merge to form one quasi-quadruplet. Below ca. 260 K, all residual spin-spin coupling is quenched, such that two pairs of distinct singlets appear instead of the two pairs of multiplets (Figure 6, c).

At least two different dynamic processes seem to influence the VT NMR results. Above room temperature all protons of the nicotine ligand (except those closest to the pyridine N atom, vide infra) give rise to fairly sharp singlets, or multiplets, between δ = +2 and −4 (Figure 6, a). Between ca. 300 and 250 K considerable broadening affects these signals (see Figure 6, b). On the other hand, after the recovery of these resonances to fairly sharp singlets (between δ ≈ 0 and −20), in particular two of the low-field singlets of the indenyl ligands are broadened considerably (see Figure 6, c). At the lowest accessible temperature (183 K), four of the seven indenyl resonances merge to form one broad singlet (not shown in Figure 6).

Interestingly, the chemical shifts of all indenyl resonances of **3** vary only slightly with temperature. In contrast, the α-protons of the substituted pyridine unit (see Figure 1) give rise to just one broad singlet at δ ≈ −16 at 353 K and to two broad signals at δ ≈ −65 and −75 at 188 K. This indirectly suggests that the magnetic susceptibility of the central Pr^{3+} ion of **3** should increase considerably with decreasing temperature. The singlet of the *N*-bonded methyl group of the nicotine ligand is shifted from δ = −0.85 at 353 K to δ = −8.00 at 193 K. The intermediate broadening of the nicotine resonances might be associated with the slowing down of the initially rapid (on the NMR timescale) internal motions of the nicotine molecule (e.g. the inversion of the non-planar pyrrolidine unit including that of the chiral NC_3 pyramid and/or rotation about the inter-ring C−C and N−Ln σ bonds). It should be noted that the resonances of the THF protons of the previously reported[8] adduct [Pr(Ind)$_3$·THF] show notable broadening between ca. 290 and 260 K (Figure 7), a feature which could be associated with ring inversion or restricted rotation about the O−Pr bond. Moreover, the temperature dependence of the indenyl resonances of this adduct is considerably less pronounced than that of the THF protons (Figure 8).

The unexpected broadening of the indenyl resonances of **3** below ca. 250 K most probably reflects some rapid intramolecular dynamics other than the bare rotation of each η^5-coordinated ligand about its Pr−C*ti*5 axis. We have speculated earlier[10] on periodic η^5-to-η^1 conversions affecting each of the three indenyl units equally and stereoselectively such that during this sequence of equilibria, the chiral intermediate η^1-coordinated C_5 ring carbon atom (i.e. C-1 or C-3) of each C_9H_7 ligand would maintain only one distinct configuration. Unfortunately, our present VT NMR spectroscopic study does not include results for temperatures around and below the coalescence of the dynamics, since the solvent starts crystallising below 180 K.

Most of the resonances of the indenyl protons of complex **4** (Ln = Nd) could be identified (Figure 4, b). A comparison with corresponding data for three previously reported adducts (Table 5) strongly suggests that the indenyl protons of **4** are also affected by the asymmetry of the nicotine ligand. While spin-spin coupling can be suggested as an explanation for the "doublet" character of the resonances assigned to protons in the positions 4/7 and 5/6, the assignment of the singlet at δ = 1.74 to 2-H (see Table 5) remains somewhat more uncertain. Alternatively, this signal might be assigned to the *N*-bonded methyl group of the nicotine ligand. The two equally intense signals at δ = −4.73 and −5.88 seem to be shifted too greatly by the paramagnetism of the Nd^{3+} ion, to justify the correlation of one of them

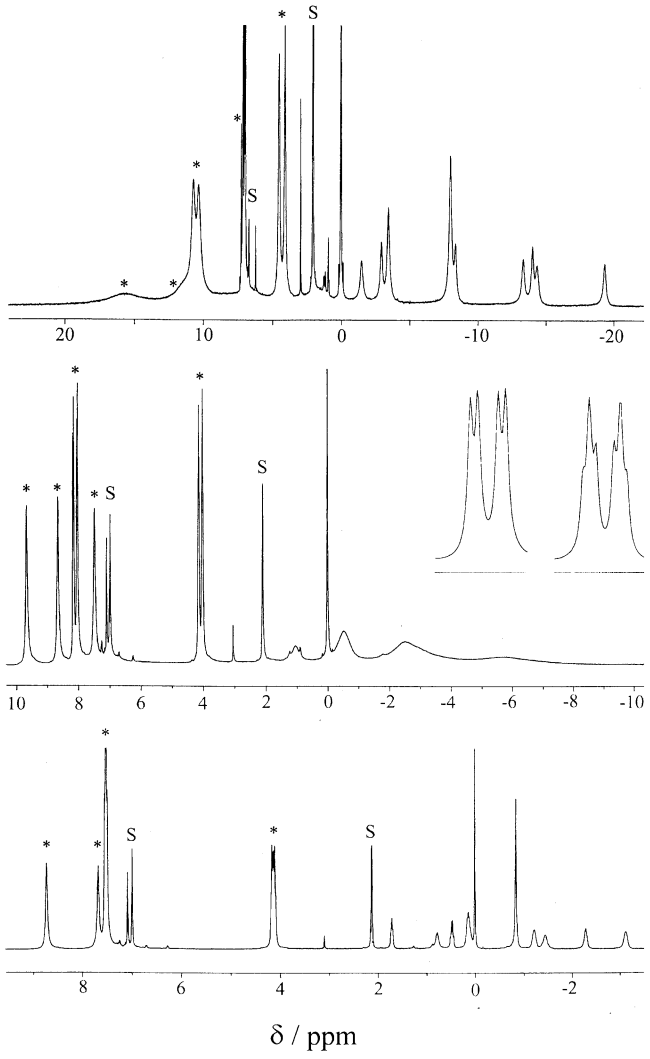

Figure 6. VT ^{1}H NMR spectra of **3** (solvent S: $CD_3C_6D_5$/TMS) at (from top to bottom) 193, 293 and 353 K; signals of the indenyl protons are marked by asterisks; the insert (for 293 K) shows the resonances of the indenyl protons 4/7-H and 5/6-H at an expanded δ scale; the spectra at 193 and 353 K do not include two additional nicotine resonances beyond δ = −20 and −4, respectively

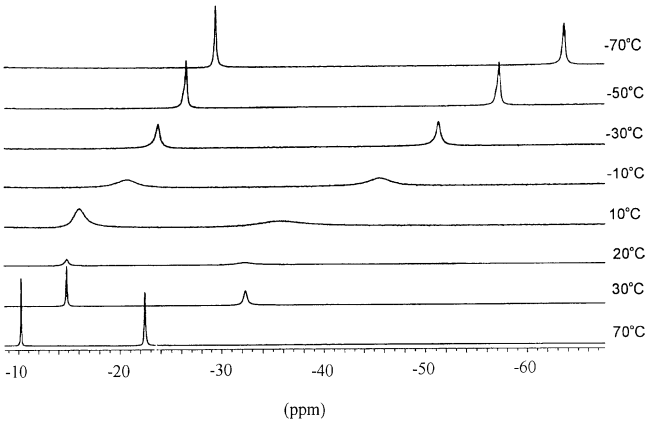

Figure 7. VT ^{1}H NMR spectra of the two THF resonances of [Pr(Ind)$_3$·THF] (solvent: $CD_3C_6D_5$)

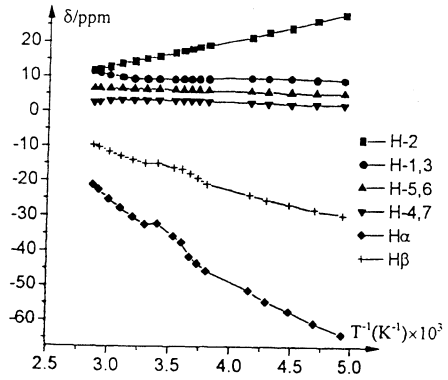

Figure 8. δ-vs-T^{-1} plots of all proton resonances of [Pr(Ind)$_3$·THF] (solvent: $CD_3C_6D_5$); the "humps" in the curves for Hα and Hβ (of THF) occur in the temperature range of pronounced line broadening (see Figure 7)

with the NCH_3 protons which are separated from the paramagnetic centre by *six* atoms. Equally far away from the metal ion are two of the CH_2 groups of the pyrrolidine unit (see Figure 1), the δ values of which should lie between δ = −2 and +2. Assuming that the signals at δ = −4.73 and −5.88 actually belong to the indenyl protons 1-H and 3-H (Figure 5, b, and Table 5), the experimentally found relative intensities of the six well-identified indenyl resonances (i.e. I_{rel} = 2 × 3, 2 × 3, 3, 3) simply require that one of the three appropriately intense signals at δ = 1.8, 0.2, or −0.8 be assigned to the proton 2-H.

f-f Circular Dichroism of 3 and 4

We have demonstrated recently that the 1:1 adducts of [Pr(Ind)$_3$] and (*R*)-(+)- and (*S*)-(−)-MTSO display, in the visible spectral range, significant circular dichroism (CD) of distinct f-f ligand-field excitations. However, the corres-

Table 6. Circular dichroism of [Pr(Ind)$_3$·(*R*)-(+)-MTSO][10] and [Pr(Ind)$_3$·(*S*)-(−)-Nic] (**3**) in the spectral range: 16100−21800 cm^{-1}

[Pr(Ind)$_3$·(*R*)-(+)-MTSO][a]		[Pr(Ind)$_3$·(*S*)-(−)-Nic][b]	
ν[c]	$10^4 \times \Delta\varepsilon_m$[d]	ν[c]	$10^4 \times \Delta\varepsilon_m$[d]
16155	−4.2		
16313	8.5		
16539	9.1		
		18677	4.8
		18890	−5.3
		19075	1.1
		19208	−1.7
		19402	2.7
19817	−30.6	19708	−2.6
		19972	−2.1
20226	16.6	20121	1.0
		20259	−1.7
20429	23.5	20429	6.8
20593	−16.9		
20781	7.4	20721	5.9
20964	−14.8	20964	−5.0
21177	1.6	21367	2.5
21758	53.7	21739	21.7

[a] $c(Pr^{3+})$ = 2.358·10^{-2} mol·L^{-1}. − [b] $c(Nd^{3+})$ = 1.298·10^{-2} mol·L^{-1} (solvent: C_6H_6). − [c] Dimension: cm^{-1}. − [d] Dimension: L·mol^{-1}·cm^{-1}.

ponding adducts involving [$PrCp_3$] and chiral MTSO were found to be practically CD-silent.[10] The new adduct [$Pr(Ind)_3$·(*S*)-(−)-Nic] (**3**) is CD-active as well, although its $|\Delta\varepsilon_m|$ values throughout are notably smaller than those reported for the MTSO adducts (see Table 6). In particular, f-f ligand excitations of **3** to states resulting from the $^1D_2$ manifold of the free Pr^{3+} ion (between ca. 16000 and 17000 cm^{-1}), which are predicted (and known) to be chiroptically less sensitive than excitations of states originating from ^3P_J manifolds with $J = 0$, 1, and 2,[18] are strictly CD-silent. The surprisingly large $\Delta\varepsilon_m$ values of both homologues around ca. 21700 cm^{-1} are probably due to an appreciable non-4f orbital admixture to the wave functions of the excited states. According to some qualitative studies (not considering the exact concentration of the dissolved sample), the neodymium homologue **4** also displays notable f-f CD. In Figure 9, the CD spectrum of **4** between 14500 and 20000 cm^{-1} is compared with the regular f-f-absorption spectrum for that spectral range.

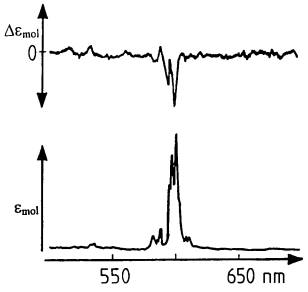

Figure 9. Absorption spectrum (bottom) and circular dichroism (top) of **4** (Ln = Nd) between 500 and 700 nm

Conclusions

According to the present study, only a relatively small selection of pyridine derivatives (Py*) is capable of occupying the vacant coordination site of an {$Ln(Ind)_3$} fragment, probably due to steric reasons. The nicotine molecule [i.e. 1-methyl-2-(3-pyridyl)pyrrolidine] *is* found to coordinate exclusively via its pyridine N atom, although *N*-methylpyrrolidine is known to combine with several {$LnCp_3$} fragments.[5] To the best of our knowledge, no crystal structure analysis of the generally liquid, free ligand has thus far been reported. The nicotine molecules coordinated in **2**, **3**, and **4** display a conformation very similar to that recently described[19] for a purely organic adduct, based upon O−H···N(Nic) hydrogen bonds.

The systematic assessment of the relevant crystallographic results for all new [$Ln(Ind)_3$·Py*] complexes supplements and confirms our earlier findings[7−10] in which the {$Ln(Ind)_3X$} fragment can adopt a large variety of mainly chiral conformations, wherein the benzo group of each indenyl ligand may be oriented either partially *meridionally* and partially *equatorially*, or all-*equatorially*. The latter situation is usually preferred as the ionic radius of the Ln^{3+} ion decreases.

By making use of the earlier described (for different types of complexes)[20] considerable amplification of the splitting of the resonance lines of initially prochiral nuclei by the auxiliary paramagnetism of Ln^{3+} ions with appropriate $4f^q$ configurations, the recognition of the remote chirality centre on the (*S*)-(−)-nicotine ligand by the indenyl protons could be readily achieved. Moreover, the 4f electrons of the ions Pr^{3+} (in **3**) and Nd^{3+} (in **4**) are capable of monitoring a chirogenic centre even more directly, such that various f-f ligand field transitions display weak, but significant circular dichroism, already at room temperature. Some very rapid (on the NMR timescale) and incompletely observable intermolecular reorganisation affecting essentially the indenyl ligands, is likely to imply a short-lived low-temperature modification of **3** involving another chirogenic centre, notably closer to the central metal ion than the dissymmetric carbon atom of the nicotine ligand.

Experimental Section

General Methods: All experimental manipulations, including sample preparation for instrumental measurements, were carried out under N_2 using vacuum-line and Schlenk techniques. The starting compound [$La(C_9H_7)_3$·THF] was prepared as described previously.[13] The nitrogen bases used were commercially available (Aldrich or Merck). − Infrared spectra were obtained with a Perkin−Elmer IR-1720 spectrometer. − ^1H NMR studies were carried out either with a Varian Gemini 200 (^1H, room temperature, solvent: [D_6]benzene) or with a Bruker AM 360 spectrometer (^1H-VT and ^{139}La-VT). Solvents for the VT studies were either [D_8]toluene (^1H) or a 3:7 mixture of [D_8]toluene and toluene and a 3:7 mixture of CD_2Cl_2 and CH_2Cl_2. ^{139}La NMR studies required the use of 10-mm NMR tubes under the following conditions: deuterium lock, SI = 4 K, TD = 8 K, SW = 71 kHz, DW = 7.0 μs, AQ =0.05s, NS = 825. A solution of either [$LaCp_3$·DMSO] in CD_2Cl_2 or of $LaCl_3$ in D_2O was used as an external standard. − Mass spectra were recorded with a Varian 3MA instrument with a spectrosystem MAT 188 (Finnigan) detector. The samples were prepared in carefully conditioned glass capillaries that could be fixed exactly on the head of the sample device, and were connected directly with the sample oven as soon as the capillary was cut off. − Optical (NIR/Vis) absorption spectra were recorded with a Cary 5E instrument, and the f-f CD spectra with a Jasco J 500 G dichrograph equipped with a DP-500 N data processor. The differential molar extinction values $\Delta\varepsilon_m$ were determined according to ref.[21]

X-ray Crystallography: Data collections were performed with a Hilger−Watts Y290 diffractometer at 153 K (Tables 7 and 8). All X-ray work was carried out with Mo-K_α radiation (λ = 70.926 pm) with the ω/2θ-scan technique. All calculations were based on SHELX-93 and SHELXTL-PLUS programme sets.[22] Heavy atoms were found from Patterson maps, and other non-hydrogen atoms were detected by Fourier techniques. Refinement was based on full-matrix least-squares techniques. Hydrogen atoms were included by use of a riding model with d(C−H) = 96 pm. $R1 = \Sigma||F_o| - |F_c||/\Sigma|F_o|$; $wR2 = [\Sigma w(F_o^2 - F_c^2)^2]/\Sigma w(F_o^2)^2]^{1/2}$; $S = [\Sigma w(F_o^2 - F_c^2)^2/\Sigma(n - P)]^{1/2}$; $P = [\max(F_o^2, 0) + 2F_c^2]/3$. Further details on the crystal structure investigations may be obtained from the Fachinformationszentrum Karlsruhe, D-76344 Eggenstein-Leopoldshafen, Germany [Fax: +49-7247/808-666; E-mail: crysdata@fiz-karlsruhe.de], on quoting the depository numbers CSD-380205 (**2**), -380204 (**3**), -380206 (**4**), -410174 (**5**), and -380201 (**6**).

Table 7. Survey of crystal data and details of data collection and refinement for the complexes **2**, **3**, and **4**; diffractometer: Hilger & Watts Y290; temperature: 153K

	2	**3**	**4**
Empirical formula	$C_{37}H_{35}LaN_2$	$C_{37}H_{35}N_2Pr$	$C_{37}H_{35}N_2Nd$
Wavelength [pm]	71.037	71.037	71.037
Space group	$P2_1$	$P2_1$	$P2_1$
a [pm]	1446.2(5)	1071.3(9)	877.1(4)
b [pm]	916.7(10)	2080(2)	2527.5(7)
c [pm]	2187(3)	1289(3)	1376(2)
β [°]	92.50(4)	91.96(11)	102.04(8)
V [nm^3]	2.896	2.871	2.984
Z	4	4	4
Density (calcd.) [gm^{-3}]	1.483	1.450	1.451
Absorption coefficient [mm^{-1}]	1.503	1.723	1.768
F(000)	1312	1280	1324
θ range for data collection [°]	2.29−30.06	2.43−25.06	2.37−27.57
h	−7 to 20	−12 to 12	−2 to 11
k	−4 to 12	−24 to 0	−5 to 32
l	−30 to 30	0 to 15	−17 to 17
Reflections collected	10633	5658	9993
Independent reflections (R_{int})	9545 (0.0199)	5248 (0.0423)	7366 (0.0460)
Data/restraints/parameters	9542/1/723	5248/1/723	7312/1/711
Goodness of fit on F^2	1.034	1.051	1.087
Final *R*1/*wR*2 indices [$I > 4\sigma(I)$]	0.0292/0.0647	0.0367/0.0974	0.0597/0.1052
*R*1/*wR*2 (all data)	0.0389/0.0694	0.0395/0.0996	0.1182/0.1421
Flack parameter	0.01(2)	0.04(3)	0.07(5)
Largest diff. peak and hole [e·nm^{-3}]	1730 and −861	1474 and −1382	479 and −744

Table 8. Summary of crystal data and details of data collection and refinements for **5** and **6**; diffractometer: Hilger & Watts (Y290); temperature: 153 K

	5	**6**
Empirical ormula	$C_{32}H_{26}NPr$	$C_{33}H_{28}NPr$
Wavelength [pm]	71.073	71.073
Space group	*Pbca*	*Pbca*
a [pm]	1376.3(3)	1163.6(4)
b [pm]	1301.5(3)	1493.7(7)
c [pm]	2631.0(5)	2940.1(13)
V [nm^3]	4.713(2)	5.110(4)
Z	8	8
Density (calcd.) [gm^{-3}]	1.594	1.506
Absorption coefficient [mm^{-1}]	2.089	1.928
F(000)	2272	2336
θ range for data collection [°]	2.29−27.54	2.32−30.15
h	−1 to 14	−2 to 16
k	−1 to 16	−2 to 21
l	−33 to 33	−2 to 41
Reflections collected	10826	10592
Independent reflections (R_{int})	4658(0.0401)	7251(0.0354)
Data/restraints/parameters	4649/0/307	7201/0/317
Goodness of fit on F^2	1.083	1.047
Final *R*1/*wR*2 indices [$I > 2\sigma(I)$]	0.0339/0.0912	0.0470/0.1175
*R*1/*wR*2 (all data)	0.0384/0.0971	0.0603/0.1455
Largest diff. peak and hole [e·nm^{-3}]	903 and −1051	2645 and −1641

Tris(cyclopentadienyl)[(*S*)-(−)-nicotine]lanthanum, [La(C_5H_5)$_3$·Nic] (1): A solution of (*S*)-(−)-nicotine (0.47 g, 2.93 mmol) in toluene (5.2 mL) was added to a suspension of [La(C_5H_5)$_3$·THF] (1.19 g, 2.93 mmol) in toluene (20 mL). After stirring (1 d) and filtration, the yellowish filtrate was concentrated and cooled to 0 °C. After washing (hexane) and drying (vacuum), the resulting precipitate was a colourless powder (yield: 1.32 g, ca. 91%; m.p. 165−170 °C). − $C_{25}H_{29}LaN_2$ (496.43): calcd. C 60.52, H 5.84, N 5.64; found C 59.67, H 5.88, N 5.84. − MS; *m*/*z*: 334, 269, 204, 162, 133, 119, 105, 83, 78 for [Cp$_n$La]$^+$ (*n* = 3, 2, 1); [nicotine]$^+$, [$C_5H_4NC_4H_7$]$^+$, [$C_5H_4NC_3H_5$]$^+$, [$C_5H_4NC_2H_3$]$^+$, [C_5H_4N]$^+$, [$C_4H_6NCH_3$]$^+$, [C_5H_5]$^+$. − ^{1}H NMR (C_6D_6/TMS, first-order as-

sessment, note that the signal assignment for the nicotine protons follows the designation chosen in Figure 1): δ = 6.13 (s, 15 H, Cp), 8.81 (s, 1 H, a), 8.30 (d, J = 5.16 Hz, b), 7.22 (d, J = 7.82 Hz, d) 6.57 (pseudo-q, 1 H, c), 2.96 (t, $J \approx$ 7.0 Hz, e) 2.68 and 1.99 (t, 1 H each, $J \approx$ 8.0 H, f) 1.95 (s, 3 H, NCH_3), 1.75, 1.39 (m, 2 H each, g/h). − ^{139}La NMR (in toluene, vide supra: see Table 1).

Tris(indenyl)[(*S*)-(−)-nicotine]lanthanum, [La(C$_9$H$_7$)$_3$·Nic] (2): A solution of (*S*)-(−)-nicotine (0.61 g, 3.76 mmol) in toluene (8.0 mL) was added at room temperature to a suspension of [La(C$_9$H$_7$)$_3$·THF] (2.09 g, 3.76 mmol) in toluene (30 mL). An almost transparent solution resulted which subsequently became turbid. The mixture was stirred overnight and finally heated to 70−80 °C. After filtration, when still warm, the solvent was removed from the yellow filtrate (in vacuo), after which a viscous yellow-orange residue was obtained. After addition of a trace amount of toluene, most of this residue converted overnight partially to yellow crystals and partially to a solid "gum". The solid product (including the crystals, some of which were suitable for X-ray studies) was washed with hexane and dried at room temperature. In total, 2.30 g (95%) of **2** was obtained. M.p. 94−98 °C. − $C_{37}H_{35}LaN_2$ (646.61): calcd. C 68.76, H 5.42, N 4.33; found C 68.51, H 5.47, N 4.45. − MS; *m*/*z*: 484, 369, 254, 115, 162, 133, 119, 84 for [Ind$_n$La]$^+$ (n = 3, 2, 1), [Ind]$^+$, [Nic]$^+$, [C$_5$H$_4$NC$_4$H$_7$]$^+$, [C$_5$H$_4$NC$_3$H$_5$]$^+$, [C$_4$H$_7$NCH$_3$]$^+$. − ^{1}H NMR (C$_6$D$_6$, TMS, first-order assessment): nicotine protons: δ = 8.17 (s, 1 H, a), 7.74 (d, J = 5.26 Hz, b), 7.26 (d, $J \approx$ 7.84 Hz, d), 6.56 (pseudo-q, $J \approx$ 5.20 and 2.62 Hz, c), 3.02 (t, $J \approx$ 8 Hz, e), 2.79 and 2.06 (t, 1 H each, $J \approx$ 8.0 Hz, f), 1.86 (m, 2 H, h), 1.49 (m, 2 H, g), 2.02 (s, 3 H, NCH_3); indenyl protons: δ = 7.46 (m, 6 H, 4,7-H), 6.94 (q, 6 H, $J \approx$ 3.0 Hz, 5,6-H), 6.14 (t, 3 H, $J \approx$ 3.30 Hz, 2-H), 5.90 (s, 6 H, 1,3-H). − ^{139}La NMR (in toluene, vide supra): see Table 1.

Tris(indenyl)[(*S*)-(−)-nicotine]praseodymium, [Pr(C$_9$H$_7$)$_3$·Nic] (3): The procedure resembled the synthesis of **2**, in that [Pr(C$_9$H$_7$)$_3$·THF] (2.64 g, 4.73 mmol) in toluene (30 mL) was treated with (*S*)-(−)-nicotine (0.77 g, 4.72 mmol) in toluene (8.5 mL). An analytically pure, yellow-green, viscous oil was obtained (yield: ≥ 85%). The oil was dissolved in a small amount of toluene, after which a large amount of hexane was added. The oil slowly converted into a yellow solid that was finally isolated and dried. Leek-green crystals suitable for an X-ray crystallographic study were obtained from a hot solution of this solid in toluene (the initially clear solution was slowly cooled down to room temperature). M.p. 129−132 °C. − $C_{37}H_{35}N_2Pr$ (648.61): calcd. C 68.54, H 5.39, N 4.32; found C 68.09, H 5.55, N 4.43. − MS; *m*/*z*: 486, 371, 256, 141, 115, 162, 133, 84 for [Ind$_n$Pr]$^+$ (n = 3, 2, 1, 0), [Ind]$^+$, [Nicotine]$^+$, [(C$_5$H$_4$N)(C$_4$H$_7$)]$^+$, [C$_4$H$_7$NCH$_3$]$^+$. − ^{1}H NMR (C$_6$D$_6$/TMS): nicotine protons a−d: δ = −32.80 (s, 1 H), −30.10 (s, 1 H), −6.74 (s, 1 H), −6.21 (s, 1 H); e−h: −5.77 (s, 1 H), −3.41 (s, 2 H), −0.75 (m, 2 + 1 H); NCH_3: δ = −2.85 (s, 3 H); indenyl protons: 1/2/3-H: δ = 9.59 (s, 3 H), 7.44 (s, 3 H), 8.79 (s, 3 H); 4/7-H: δ = 8.15 (d, 3 H, J = 7.52 Hz), 8.03 (d, 3 H, J = 7.54 Hz); 5/6-H: δ = 4.19 (t, 3 H), 4.06 (t, 3 H).

Tris(indenyl)[(*S*)-(−)-nicotine]neodymium, [Nd(C$_9$H$_7$)$_3$·Nic] (4): A procedure similar to that for the preparation of **2** was adopted, using [Nd(C$_9$H$_7$)$_3$·THF] (1.68 g, 2.99 mmol) in toluene (20 mL) and (*S*)-(−)-nicotine (0.48 g, 2.98 mmol) in toluene (5.0 mL). A red-green, analytically pure, viscous oil was obtained (1.34 g, 68.7%), which was redissolved in warm toluene. After addition of a small amount of hexane, and on slow cooling, green single crystals suitable for X-ray crystallographic studies were obtained. M.p. 112−116 °C. − $C_{37}H_{35}N_2Nd$ (651.94): calcd. C 68.20, H 5.37, N 4.29; found C 67.75, H 5.41, N 4.28. − MS; *m*/*z*: 489, 372, 259, 115, 162, 133, 84 for [Ind$_n$Nd]$^+$ (n = 3, 2, 1), [Ind]$^+$, [Nic]$^+$, [C$_5$H$_4$NC$_4$H$_7$]$^+$, [C$_4$H$_7$NCH$_3$]$^+$. − ^{1}H NMR (C$_6$D$_6$/TMS): nicotine protons: a−d: δ = −14.30 (s, 2 H), −13.40 (s, 1 H), −2.95 (s, 1 H); e−h: δ = −1.89 (s, 1 H), −1.15 (s, 1 H), 0.13 (s, 2 H), 0.42 (m, 1 H), 1.50 (br, 1 H); NCH_3: δ = −0.76 (s, 3 H); indenyl protons: δ = −5.88, −4.73 (s, 3 H each, 1,3-H), 1.74 (s, 3 H, 2-H), 7.40 (d, 6 H, 4,7-H), 5.00 (d, 6 H, 5,6-H).

Tris(indenyl)(pyridine)praseodymium, [Pr(C$_9$H$_7$)$_3$·Py] (5): The preparative procedure resembled those described before. A solution of pyridine (0.16 g, 2.07 mmol) in toluene (7 mL) was added to a suspension of [Pr(C$_9$H$_7$)$_3$·THF] (1.08 g, 1.93 mmol) in toluene (30 mL) at room temperature. After workup, 1.07 g (98%) of leek-green single crystals was collected. M.p. 199−203 °C. − $C_{32}H_{26}NPr$ (565.47): calcd. C 67.99, H 4.60, N 2.47; found C 67.17, H 4.69, N 2.49. − MS; *m*/*z*: 486, 372, 256, 141, 116, 78 for [Ind$_n$Pr]$^+$ (n = 3, 2, 1, 0), [Ind]$^+$, [Py]$^+$. − ^{1}H NMR(C$_6$D$_6$, TMS): indenyl protons: δ = 10.03 (s, 6 H, 1,3-H), 8.98 (s, 3 H, 2-H), 7.88 (s, 6 H, 5,6-H), 3.65 (s, 6 H, 4,7-H); pyridine protons: δ = −4.30 (s, 1 H, H-γ), −7.66 (s, 2 H, H-β), −33.42 (s, 2 H, H-α).

Tris(indenyl)(3-methylpyridine)praseodymium, [Pr(C$_9$H$_7$)$_3$·3-MePy] (6): As for the preparation of **5**, a solution of 3-methylpyridine (0.186 g, 2.01 mmol) in toluene (10 mL) was added to a suspension of [Pr(C$_9$H$_7$)$_3$·THF] (1.12 g, 2.06 mmol) in toluene (30 mL). 1.17 g (100%) of a crystalline product was obtained. M.p. 135−138 °C. − MS; *m*/*z*: 486, 372, 256, 116, 93, 78 for [Ind$_n$Pr]$^+$ (n = 3, 2, 1), [MePy]$^+$, [Py]$^+$. − $C_{33}H_{28}NPr$ (579.50): calcd. C 68.42, H 4.83, N 2.42; found C 68.03, H 4.94, N 2.42. − ^{1}H NMR (C$_6$D$_6$/TMS): indenyl protons: δ = 10.13 (s, 6 H, 1,3-H), 8.12 (s, 6 H, 5,6-H), 7.66 (s, 3 H, 2-H), 3.68 (d, 6 H, J = 3.30 Hz, 4,7-H); 3-methylpyridine protons: δ = −4.38 (s, 1 H, Hγ), −6.67 (s, 3 H +1 H), CH_3 + Hβ), −38.9, −30.0 (s, 1 H each, Hα)

Acknowledgments

J.-W. G. would like to express his gratitude to the Friedrich-Ebert-Stiftung (Bonn) for a fellowship. We also express our deep thanks to Mrs. S. Samba for technical assistance.

[1] E. C. Baker, K. N. Raymond, *Inorg. Chem.* **1977**, *16*, 2710−2714.
[2] G. B. Deacon, B. M. Gatehouse, S. N. Platts, D. L. Wilkinson, *Aust. J. Chem.* **1987**, *40*, 907−914.
[3] H. Breitbach, Doctoral Dissertation, Universität Hamburg, Germany **1987**, p. 42 {crystal structure of [Pr(CH$_3$C$_5$H$_4$)$_3$·γ-picoline]; Pr−N distance: 264.1(4) pm}.
[4] A. Zazzetta, A. Grew, *Acta Crystallogr., Sect. B* **1979**, *35*, 457−460.
[5] R. von Ammon, B. Kanellakopulos, R. D. Fischer, P. Laubereau, *Inorg. Nucl. Chem. Lett.* **1969**, *5*, 315−319.
[6] R. von Ammon, R. D. Fischer, *Angew. Chem.* **1972**, *84*, 737−755; *Angew. Chem. Int. Ed. Engl.* **1972**, *11*, 675−692.
[7] J. Guan, R. D. Fischer, *J. Organomet. Chem.* **1997**, *532*, 147−157.
[8] J. Guan, Q. Shen, R. D. Fischer, *J. Organomet. Chem.* **1997**, *549*, 203−212, and further references given therein. Unfortunately, in Table 5 of this paper, the δ(5/6-H) value of the complex [Nd(Ind)$_3$·THF] is missing a minus sign.
[9] J. Guan, R. D. Fischer, *J. Organomet. Chem.* **1998**, *564*, 167−177.
[10] J. Guan, J. Stehr, R. D. Fischer, *Chem. Eur. J.* **1999**, *5*, 1992−2003.
[11] J. Guan, Doctoral Dissertation, Universität Hamburg, Germany, **1998**: [11a] p. 49, [11b] p. 37, [11c] p. 141.

[12] S. H. Eggers, H. Schultze, J. Kopf, R. D. Fischer, *Angew. Chem.* **1986**, *98*, 631−632; *Angew. Chem. Int. Ed. Engl.* **1986**, *25*, 656−657.
[13] J. Xia, Z. Jin, G. Lin, W. Chen, *J. Organomet. Chem.* **1991**, *408*, 173−179.
[14] J. G. Brennan, S. D. Stults, R. A. Anderson, A. Zalkin, *Inorg. Chim. Acta* **1987**, *139*, 201−202.
[15] W. A. Herrmann, R. Anwander, F. C. Munck, W. Scherer, *Chem. Ber.* **1993**, *126*, 331−337.
[16] R. Anwander, W. A. Herrmann, F. C. Munck, W. Scherer, *J. Organomet. Chem.* **1993**, *462*, 163−174.
[17] D. M. Barnhart, D. L. Clark, J. C. Huffman, R. L. Vincent, J. G. Watkin, *Inorg. Chem.* **1993**, *32*, 4077−4083.
[18] F. S. Richardson, *Inorg. Chem.* **1980**, *19*, 2806−2812.
[19] See: K. Fukawa, S. Harada, N. Kasai, M. Toda, K. Mori, F. Toda, *Bull. Chem. Soc. Jpn.* **1989**, *62*, 2714−2716.
[20] A. Steudel, E. Siebel, R. D. Fischer, G. Paolucci, V. Lucchini, *J. Organomet. Chem.* **1998**, *556*, 229−238; A. Steudel, J. Stehr, R. D. Fischer, *J. Organomet. Chem.* **1998**, *570*, 89−96.
[21] H. B. Kagan, *Stereochemie*, Thieme, Stuttgart, **1979**; S. F. Mason, *Molecular Optical Activity and Chiral Discrimination*, Cambridge University Press, Cambridge **1982**; *Circular Dichroism. Principles and Applications* (Eds.: N. Berova, K. Nakanishi, R. W. Woody), Wiley-VCH, New York, **2000**.
[22] SHELX-86: G. M. Sheldrick, *Acta Crystallogr., Sect. A* **1990**, *46*, 467−473; G. M. Sheldrick, *Program for the Refinement of Crystal Structures*, Universität Göttingen, Germany, **1993**; G. M. Sheldrick, *SHELX-PLUS*, Release 4.21/v, Siemens Analytical X-ray Instruments, Madison, Wisconsin (USA), **1995**.

Received April 17, 2001
[I01134]